

HSL Color Space for Potato Plant Detection In The Field

Taher Deemyad
Department of Mechanical
Engineering Idaho State University
Pocatello, ID USA
deemtahe@isu.edu

Anish Sebastain
Department of Mechanical
Engineering Idaho State University
Pocatello, ID USA
sebaanis@isu.edu

Abstract— This research paper discusses a vision system and image processing algorithms for an autonomous vehicle to be implemented for precision agriculture purposes. This system is a part of a larger project, to detect and remove potatoes infected by a commonly occurring virus (PVY – potato virus Y). For the detection and removal of infected plants, first, an unmanned aerial vehicle (UAV) equipped with a hyperspectral camera and a high precision GPS, will fly over the potato field collecting images of the plants. Using custom image analysis, the GPS location of the sick plant is identified and sent to an autonomous ground vehicle (AGV). This AGV will then navigate to the target location and rogue the infected plant automatically. The RTK GPS used here has an error of about 10cm. After the AGV reaches the target location the automatic roguing mechanism will still need to identify the sick plant. Potato seeds are planted at an average distance of about 30 centimeters, but in reality, this distance may vary significantly in the field. To positively identify the sick plant in real-time, a special image processing system was designed to detect and position the rouging arm over the center of the sick plant. This system uses an 8 Megapixel Pi camera to find the center of the target plant looking down. This system needs to work with high accuracy in a potato field where changing sunlight and weather conditions would hamper proper identification, HSL (hue, saturation, and lightness) format of images was used for better color detection. Two methods for finding the center of the plant were compared. These were compared to positive detection rates for various light levels, a variety of leaf colors, and expected location as opposed to actual plant location.

Keywords— *Segment plants based on HSL format, Image processing, Threshold method, Detection and localization in 2D and 3D, Vision applications and systems, Agriculture image processing, Vision for robotics and autonomous vehicles*

I. INTRODUCTION

Diseases always affect the quality and quantity of farmers' products. One of the best ways to minimize loss of production in the field is early detection and removal of infected plants. [11, 13, 19]. To accurately identify infected plants, we need to identify physical manifestations of the disease [12, 27]. Detection of sick plants is cumbersome for large fields, but computer vision technologies aid in early and fast detection using leaf images [12, 1, 5, 2].

With recent improvements in the science of robotics and autonomous systems, image processing plays a more critical role for correct decision making, path planning, obstacle avoidance for mobile robots [4, 14]. Image processing is especially challenging in a farm.

Most image processing techniques focus on the size and color of objects. Most of them change the picture color of the object to gray, black and/or white formats for analysis. While loss of contrast, sharpness, shadow, and structure of the color images are some of the characteristics of converting a colored image to gray images, scientists are working on improving this method [20, 25]. However, in a field, based on weather conditions, a wide range of illumination of the surface of the plant by sunlight creates different levels of shadows and changes the lightness of the picture [7, 23]. Also, there is the possibility of unexpected objects, like farm equipment which might further change the image of the leaves on the farm. Plus, the size of the target objects can be different, as fruits and vegetables vary in size and shape [26, 22].

Image processing could be applied to black and white or gray pictures or one could work with color pictures too (Red-Green-Blue, RGB). The problem with colored images is we have to work with three variables which makes it complicated. Two other alternatives are converting the picture to HSL (hue, saturation, lightness) and HSV (hue, saturation, value) [21, 8, 18].

Using the HSL color space for detection of a range of colors, for instance, detection of colors in yarn-dyed fabrics [17] or for agricultural purposes (detection of fruits and vegetables) can be an excellent choice [16]. MATLAB has a user-friendly environment for coding, especially for image processing. In [9], a combination of Internet of Things (IoT) and Image processing in the field of agriculture was discussed.

With recent improvements in electronics and programming software, a combination of machine vision and image processing techniques provides a promising implementation for accurate real-time plant detection in the field [24, 10]. In the current research, one of the novel methods for infected plant detection, using a ground-vehicle's onboard machine vision and image processing techniques is presented and discussed.

In field of agriculture for detecting of plants in the field there are lots of research using pixel-wise classification. In [31] deep convolutional neural networks for semantic segmentation of cluttered classes in RGB images was analyzed. In [32], a detection system with using a camera installed on a mobile field robot for detecting sugar beet plants and weeds was studied. In [33] the convolutional neural networks (CNNs) was applied to the RGB and near infra-red (NIR) images for the crop/weed detection.

This study is important for improving the protection of agricultural products against the viruses. On the other hand in

this study, we working on an image processing for detecting plants in a wide range of natural light with using a completely automatic detection system, This system works based on some initial data from GPS system and a novel image processing algorithm for finding the center of target plant in different situation.

II. PROJECT OVERVIEW AND CONDITIONS OF THE TARGET ENVIRONMENT

The research topic presented here is part of a larger project for the detection and removal of potatoes infected by the virus Y autonomously. The complete process for this system is presented in Fig. 1. A quadcopter (UAV) equipped with a hyperspectral camera and Real-Time Kinematic (RTK) (high accuracy GPS) flies over the field taking images. After analyzing these images the location of sick plants is identified in the field. The GPS coordinates for these target plants are then sent to an Autonomous Ground Vehicle (AGV). This AGV will be built over an optimized chassis based on a prototype chassis designed by Deemyad et al. [3] The AGV will be outfitted with an appropriate roguing mechanism [28]. This roguing mechanism was selected based on the strengths of the grasping mechanisms with a minimum number of actuators [29, 30]. Also, this AGV can navigate using an onboard obstacle avoidance system [15]. However, once the AGV navigates to the specified location, the problem at this stage is identifying the exact center point of the sick plant (looking down on the plant). This is extremely important to extract the sick plant completely from the ground, without contaminating nearby ones. But even in the most accurate GPS (RTK GPS with just 10cms error), there is always an uncertainty involved. Therefore, to solve this problem, once the rover reaches the intended location the target plant will be positively identified using two cameras, and an image processing algorithm to find the center of the sick plant.

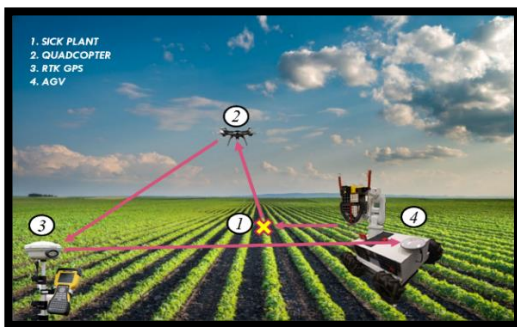


Fig. 1. Guiding Autonomous Ground Vehicles (AGV) to the target location by sending GPS coordinate from the Unmanned Air Vehicles (UAV).

Before working on a specific image processing algorithm, we needed to collect additional details of the environment (potato field) and specifications related to the target object (potato plant). To get preliminary environment information we visited a local potato field and based on our observations, collected three major sets of data. First of all, this system is supposed to work in an open area where weather conditions are unpredictable. One of the most important and commonly occurring change, is in the amount of sunlight during the day. This could be due to any number of reasons; for example – clouds in the sky, shadows in the field, etc. This would have a direct impact on the type of image processing algorithm that could be used. The second point that needed consideration, relates to the color variations of the target object due to the

lighting changes and other possible dynamic elements in the surroundings. In this project, this system must detect a sick potato plant with high accuracy for removal. A potato plant, based on age, soil conditions, and weather can have a large range of variations of the color green. Some of the other common colors in the potato fields which have to be filtered are soil color, other reflected light/shadows from irrigation equipment, rocks, water on the field, etc. Another factor to bear in mind is the shape of the potato field, distance between plants, and size of the plants at the time of roguing. Based on our observations and measurements from the field visits, a simulated model of a potato field was made in SolidWorks which was used in future calculations and image processing algorithm development. This simulated model is shown in Fig. 2. As shown, a potato field is fraught with rough terrain and deep irrigation ruts. The center to center distance between the top points of the two bumps is around 60cm. The plants are grown on the top/crests of the bumps and the average distance between two plants is around 30cm along the row. The cross sign in Fig. 2, shows the target sick plant between eight healthy adjacent plants in the potato field. In this research, we are considered an ideal condition when the distance between plants are almost equal (30cm away from each other) but in reality, in a potato field, this distance can be vary and even maybe two plants are connected to each other. This would be one of the main challenges and can be solve by some changes in the extraction mechanism which will be discussed in another study.

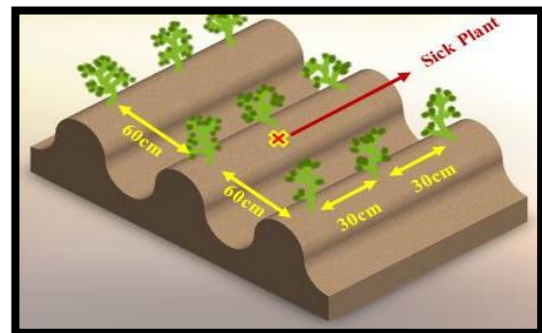


Fig. 2. Simulated potato field and an average distance between plants in the field.

Usually, PVY can be detected in potato plants very early on, in the growth cycle [6] using hyperspectral imaging. This is the best time to detect and remove the infected plants from the field before the virus spreads to other plants. However, this period is usually very short during the crop cycle. To conduct tests and to test our algorithms, we planted some potatoes indoors. We used the same pattern and shape of the field for planting a single row of potatoes. (Fig. 3).



Fig. 3. Planted potatoes indoor with similar pattern in the field.

III. EQUIPMENT AND APPROPRIATE COLOR SPACE

A. HSL Color Space

The major challenge was in developing an algorithm for correctly identifying an infected plant, in the large range of colors, all within the green domain. Therefore, using a gray or black white scale would not be a suitable option here. On the other hand, working with color spaces is usually very complex. Plus, this system has to work in outdoor conditions, again with a wide range for brightness. Between all color space models, the HSL would be an appropriate option. In this model, H, S, L are Hue, Saturation, and Lightness respectively. As previously discussed, the system needs to work in a wide range of Lightness, so we experimented with the two remaining components (Hue and Saturation) to find the most appropriate map for the target color range.

The images are taken by cameras are in RGB (Red-Green-Blue) format which has to be converted to HSL format. For this conversion, we will use the following sets of equations from [21]:

$$R' = R/255 \quad , \quad G' = G/255 \quad , \quad B' = B/255 \quad (1)$$

$$C_{max} = \max(R', G', B') \quad , \quad C_{min} = \min(R', G', B') \quad (2)$$

$$\Delta = C_{max} - C_{min} \quad (3)$$

Lightness:

$$L = (C_{max} + C_{min})/2 \quad (4)$$

Saturation:

$$S = \begin{cases} 0 & , \quad \Delta = 0 \\ \frac{\Delta}{1 - |2L - 1|} & , \quad \Delta \neq 0 \end{cases} \quad (5)$$

Hue:

$$H = \begin{cases} 0^\circ & , \quad \Delta = 0 \\ 60^\circ \times \left(\frac{G' - B'}{\Delta} \text{ mod } 6 \right) & , \quad C_{max} = R' \\ 60^\circ \times \left(\frac{B' - R'}{\Delta} + 2 \right) & , \quad C_{max} = G' \\ 60^\circ \times \left(\frac{R' - G'}{\Delta} + 4 \right) & , \quad C_{max} = B' \end{cases} \quad (6)$$

Where H, S, and L could be any values between 0-1. We set up an appropriate range for each of them based on the color range we needed to detect, this is further explained in the results section.

B. Equipment

For testing the developed algorithm, for image processing (before final installation onboard the AGV) we performed tests in a laboratory setting to ascertain the accuracy of the algorithm and make any modifications to the same. The cameras were attached to a 1/3 scale prototype model of roguing mechanism. While the roguing mechanism itself, was attached to an IRB 120 robotic arm with the ability to be

controlled manually or automatically. In the final field operational AGV, two cameras will be used to locate the roguing arm in the X and Y directions. The second camera is used for redundancy. In the lab tests, a single camera was tested.

A list of all the relevant hardware used is shown in Table I and Fig. 4.

Fig. 5 shows the location of the cameras on the prototype of the roguing mechanism. The camera looking down on the plant in the Y direction, give us a top view of the plant while the second camera would provide the front view of the plant to locate the stem. The work described here only deals with images acquired by the camera looking down on the plant to identify the plant center.

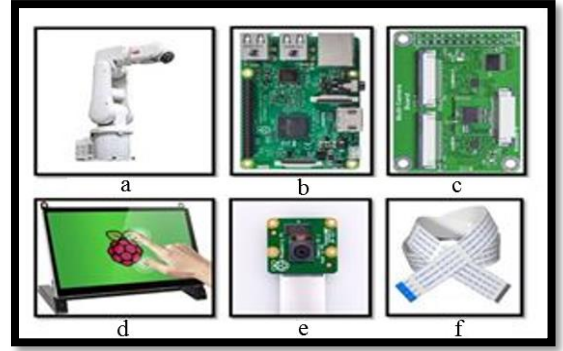


Fig. 4. Required components for image processing and detect the infected plant.

TABLE I. LIST OF EQUIPMENT.

#	Parts	Description	Qty
a	Robotic Arm	IRB 120	1
b	Micro Controller	Raspberry Pi 4 B	1
c	Multi Camera Adapter	Arducam Multi Camera Adapter Module V2.1	1
d	Monitor	Raspberry Pi Touchscreen Monitor, 7" Touch Screen	1
e	Cameras	Raspberry Pi Camera Module v2 with Sony IMX219 8-megapixel sensor	2
f	Ribbon Flex Extension Cable	1 meter	2



Fig. 5. The location of two cameras on a prototype of roguing mechanism. Camera 1 give us the top view of the plant and Camera 2 give us the front view of the plant.

IV. PROBLEM STATEMENT AND METHODS

The first problem to overcome, during algorithm development, is related to the range of colors of the target object. The color of the leaves may vary from one plant to another due to the dynamic environment of the field, which makes it hard to narrow down the approach needed to identify

the center. The second problem is related to the amount of light during the day and uncertain weather conditions. Both of these problems can be solved by defining an appropriate range for H, S, and L values. The third problem is related to small weeds with the same green color/shade which may be growing close to the target plant. These need to be ignored to reduce false positives. The issue with the weeds can be resolved by defining a threshold for the minimum size the algorithm needs to detect for the target object and ignore anything less than this size (assume as noise) in our image detection. The fourth problem and the most complicated one, is related to detecting the target plant between other adjacent plants and find the center of this plant to avoid incorrect removal.

For solving the last problem, let's take a look at the location of the sick plant and adjacent plants from the top. Fig. 6 shows an area of 60cm×60cm of the field around the sick plant. In this figure, the yellow cross in the middle of the picture is the target plant (number 5). As mentioned before, the AGV will navigate to this location using an RTK GPS with an average error of 10cm. This error boundary is shown by a red circle in this figure. However, since we are working with pixels, using a square shape would be easier. Therefore, we will define a square boundary which is shown by the blue crosses (numbered 1 to 8) in the figure. These are other possible locations that the AGV may reach, due to the RTK average position error, and assume them as the center of a target plant. For example, the two adjacent plants which are on the left and right side of the sick plant with a distance of 30cm from it.

The 60cm×60cm square was divided into nine 40cm×40cm regions as shown in Fig. 6 with yellow, red, and black colors. In this way, any of the cross points 1 to 9 would be the center of one of these regions. Therefore, regardless of the RTK GPS navigates the AGV to the correct location for the target plant (number 5) or any number 1-9 (except 5), the camera has to search the area of 40cm×40cm around that point, find the target plant and detect the center of it.

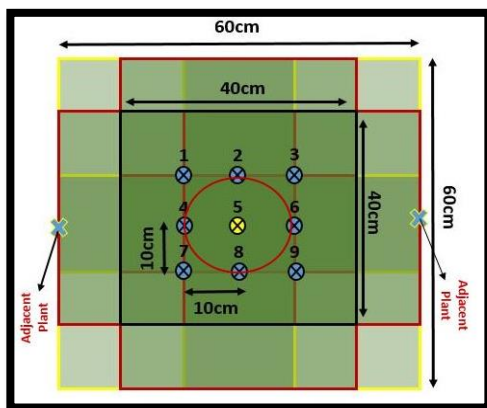


Fig. 6. The 60cm×60cm area around the target plant in the field and nine 40cm×40cm sub areas inside of this region.

As an example, let's look at one of the possible situations. Suppose point number 1 is the location sent from GPS onboard the UAV to the AGV, as the center of the target plant. We assume the distance between the camera and the ground to be fixed. The camera takes a picture from the top with the center of point 1 and a frame of 40cm×40cm. This area is shown in Figure 7. Now from this image, we have to find the

location of the target plant i.e. the center of the infected plant which is at 5.

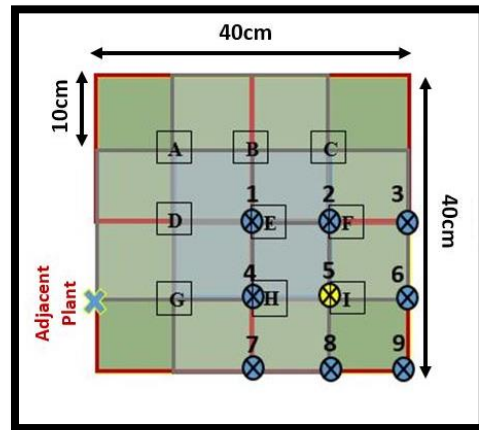


Fig. 7. The 40cm×40cm area with the center point number 1 (example).

In this case, we can use two different algorithms for finding the center of the target plant. In this section, we will explain both algorithms and in the next section, we can compare the result for each of them and select the best one.

A) In the first algorithm, the whole 40cm×40cm camera frame is divided into nine 20cm×20cm sub-frames, as shown in Fig 7 with the centers labeled from A to I. Then, the area for each of these nine regions will be calculated and the region with maximum value for the green shade will be found. Finally, the center of that region will be selected as the center of the target plant. For instance, in the example above that would be I.

B) In the second algorithm, the entire 40cm×40cm camera frame will be analyzed for green areas. Each of the connected green areas (one piece) will be selected as one blob. The area for each blob will be calculated and the largest blob will be selected as the target plant. Finally, the center of the blob would be chosen as the center of the target plant.

V. RESULTS AND DISCUSSION

As it was discussed in section IV, in this project we focus on four main aspects for accurate infected plant detection. These are color, light, size of objects, and the center of the target plant. The methods and results for each of them are presented and discussed in this section.

A. The Target Color Domain Detection

To detect the targeted plant and to isolate it from the background and other objects in a potato field, we need to find an appropriate range of the H, S, and L. After multiple iterations, an appropriate range for H, S, and L values in HSL format, for most of the possible variations of the color green for the leaves of the potato plant, was found. This is presented in Table II.


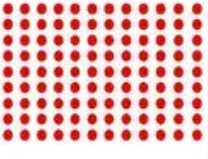


TABLE II. ACCEPTABLE RANGE OF PARAMETERS IN THE HSL FORMAT.

HSL Format	H	S	L
Minimum	0.157	0.1373	0.1176
Maximum	0.49	1	0.85

To test these ranges and check if we can detect most of the green color domain while ignoring all other colors (especially colors related to possible objects in a potato field such as rocks, soil, etc.), a wide range of green colors was selected. The selected colors for testing are presented in Table III, in the row labeled Test A. Any of these points which can be detected by the algorithm will be replaced with a red color. As you can see all of the points in the selected green color domain had been detected. On the other hand, in Test B, a variety of other colors (except green) was selected and the test was repeated. As shown in Table III, none of them were detected.

To test the results of the algorithm in a real test case, we repeated the experiment on leaves of several different plants, with various shapes, colors, and sizes. Three samples used for this iteration are shown in Fig. 8. None of these leaves belong to a potato plant. These were chosen because in the potato field, based on the time of the roguing and other field conditions the size, shape, and color of potato leaves can be different.

TABLE III. COLOR DETECTION TEST FOR A WIDE RANGE OF COLORS.

Test	Color Range	Results After Image processing
A	<u>Green Color Range</u> 	<u>Detected points are red</u> 
B	<u>Other Possible Colors</u> 	<u>Detected points are red</u> 

As can be seen, for all three cases the camera did detect the leaves of the samples perfectly with minimum error.

B. The light range

The second condition to be borne in mind is the amount of light in the potato fields. The light intensity can vary based on the time of the day or the weather conditions. A proper range of H, S, L values (in HSL format) which we found in the previous section, affects this section too. Fig. 9 presents four levels of brightness, from very bright to a very dark scenarios. The results in three conditions; very bright, normal, and dark, show the system can detect the plant with high accuracy in these tow of the three conditions as expected. In a very dark image, it can detect around 50% of the target plant. So, this system is not recommended for the very dark condition.

C. The minimum size range

In the potato field may small weeds grow close to the planted plants. This would cause an error in determining the exact center for the target plant. Therefore, we defined a minimum sirange for detecting an object, and any value less than that would be ignored by the system. In the developed code any object with less than 300 pixels will be removed from the image. In the example that is presented in Fig. 10, we used leaves of the Noble tree. As shown, some portions of it,

which in close proximity to each other was detected as one piece but the rest of it is not detected.

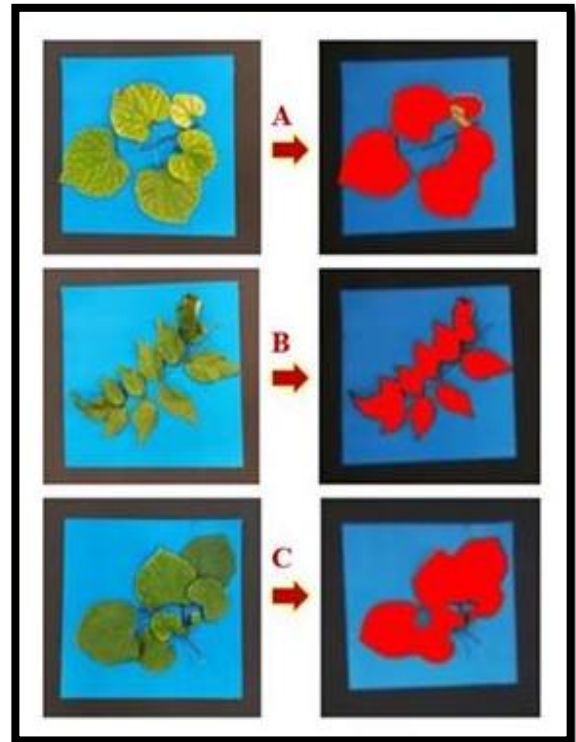


Fig. 8. Three leaves samples with different color, shape, and size to test the algorithm.

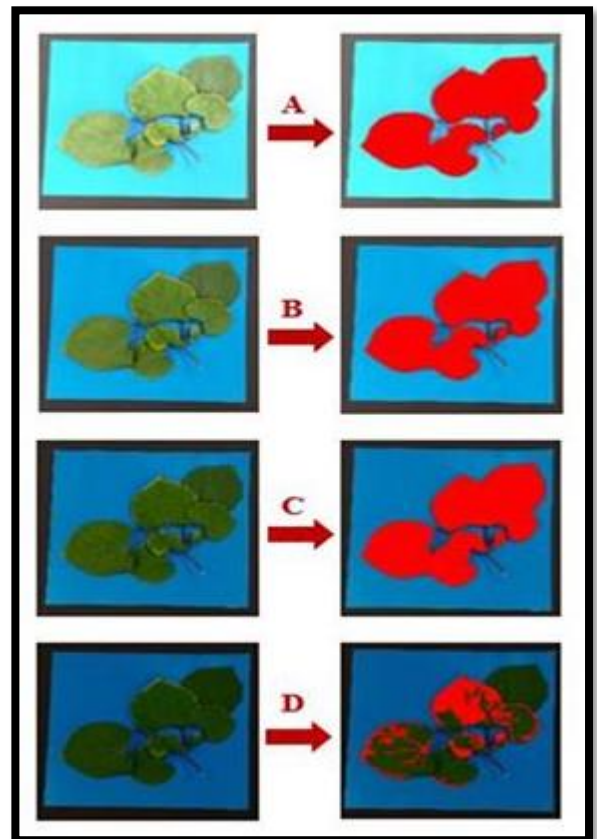


Fig. 9. Checking the accuracy of the code in various level of brightness A) very bright b) normal c) dark d) very dark.

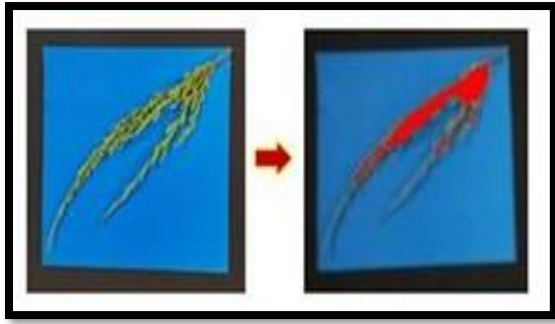


Fig. 10. The blobs with less than 300 pixel will be removed from the image.

D. Finding the center of target plant

Two algorithms were presented in the previous section for finding the center of the target plant. We tested and evaluated both methods with multiple samples. Fig. 11 shows an aerial photo of a potato field. The plant in the middle of this photo is the target plant. The yellow points show the boundary for possible coordinates which can be received from GPS and the red point (Num. 5) is the exact center of the target plant. For this test, both algorithms were tested for the worst-case scenario. The GPS sent incorrect coordinates to the AGV. This resulted in the AGV being located somewhere close to the discussed boundary, with a maximum distance from the correct center point, for example very close (but not exactly) to point Num. 9.

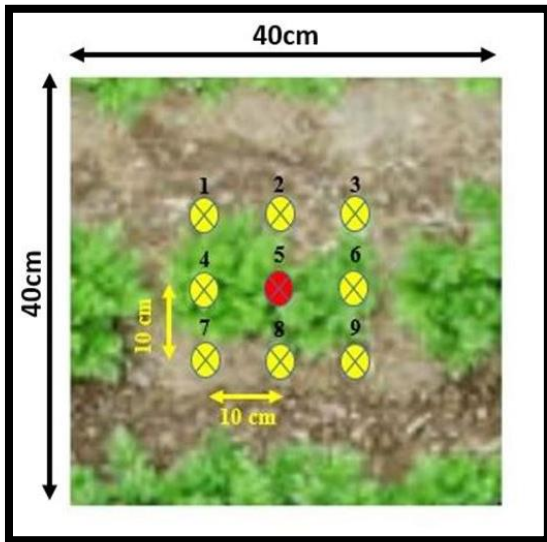


Fig. 11. Aerial photo from a potato field.

This situation is presented in Fig. 12. As you can see, this is shown an area of 40cm×40cm with the center close to point Num. 9.

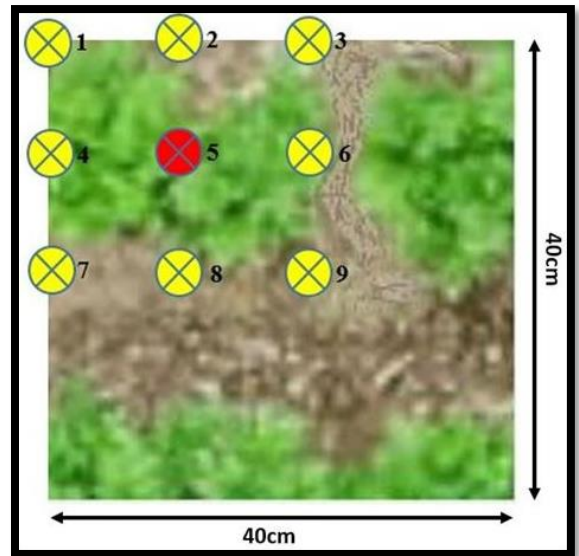


Fig. 12. The received coordinate from GPS as the center of target plant (close to Num. 9) and surrounding.

1) Results for method A

In method A, as it was explained before, the camera frame will be divided into nine equal 20cm×20cm regions. This division is shown in Fig. 13 with center points are marked A to I.

In this method, the green area for each of these regions will be calculated and the region with a maximum green area would be selected as the target region. Then, the center of that region will be selected as the center of the target plant.

Table IV shows the green parts in each region and the total green area in each of them. As it's shown, the region A with 6764 pixels has the maximum green area.

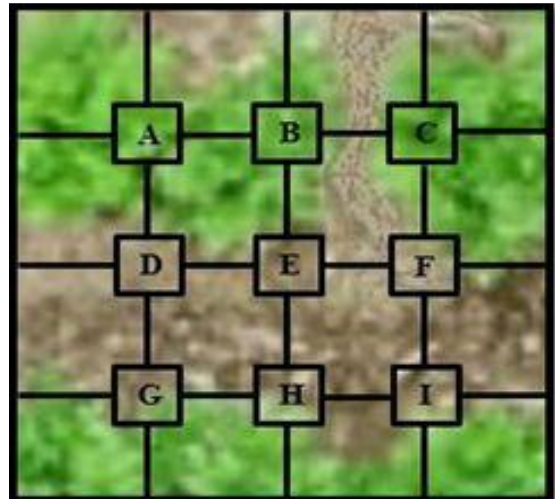











Fig. 13. Nine search regions in method A.) and surrounding.

TABLE IV. GREEN AREA FOR EACH REGION IN METHOD A.

Region A	Region B	Region C
		
6764 Pixels	5867 Pixels	6672 Pixels
Region D	Region E	Region F
		
4760 Pixels	4349 Pixels	4749 Pixels
Region G	Region H	Region I
		
4040 Pixels	3461 Pixels	3605 Pixels

2) Results for method B

In method B, the entire image will be searched to find the largest blob, and the center of it will be chosen as the center of the target plant.

The final result for both methods are shown in Fig. 14-(B) and can be compared to the true center point in Fig. 14-(A). As can be seen, both results are close to each other, with method B being slightly more accurate. In reality whenever one of those 9 points in Fig. 11, is selected as the center of the picture, method A will find the center of the target plant with 100% accuracy. However, if the selected point is in the range of 10cm but not exactly one of those points (somewhere between two of these points with less than 10cm error), method A would have an error between 0 to 5cm. On the other hand, results from method B are consistent. The results show that most of the time this method will find the center of the target plant with high accuracy.

The accuracy for each of these two methods is compared in Table 5. The error for method A, in this example, is because point 9 is not selected to be exactly in the center of the picture.

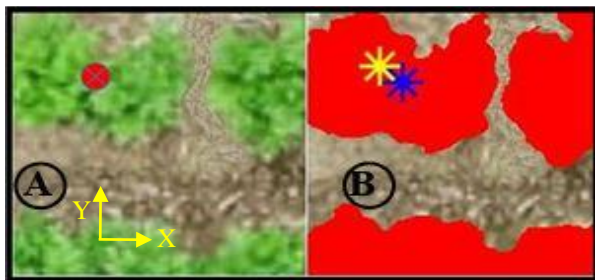


Fig. 14. A - Center of target plant; B - The center point detected from method A (yellow star) method B (blue star).

TABLE V. ACCEPTABLE RANGE OF PARAMETERS IN THE HSL FORMAT.

Center Point	X_Center (Pixel)	Y_Center (Pixel)
Method A	47.5	47.5
Method B	63	59
True Point	63	61

As you can see, the value of X and Y in method B is very close to the real center point of the target plant (only 0.4mm error in the Y direction). But method A has a larger error (around 3cm error in both directions). However, for selecting the best method between the two, we repeated the tests many times on various samples. The results for ten of them are shown in Fig. 15. In the graph green and blue lines shows the error for method A and method B for the actual center of the plant respectively. The values of these errors are presented in the table below the graph. While method A has a large fluctuation from 1cm to 5cm error, method B has a constant pattern with 1cm to 2cm error which is acceptable. For these ten tests which are shown in Fig. 15, the mean and median of error values for method A are 2.9cm and 2.8cm respectively while these values for method B, are 1.8cm and 1.9cm. So, we can say Method B in general is more accurate and reliable.

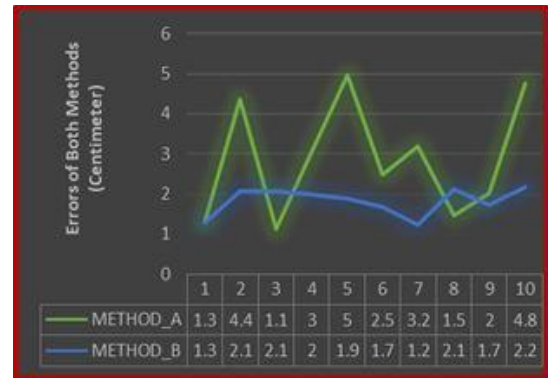


Fig. 15. Comparison between error of method A method B for ten different situations.

At the end, still there are lots of other challenges remain, such as keeping the lens of camera clean in a potato field from the dust made by driving vehicle inside of the field and keeping the distance between height of camera and a rough terrain like potato field. Also, these algorithms has been tested in the lab and we have a plan to repeat them for over 100 different cases in outside with a natural light and compare our methods with other new methods based on machine learning in the next work.

VI. CONCLUSION

In this paper, an image processing algorithm was designed and implemented for the detection of the center point of a target plant, infected with PVY in the field. In this project, first, a quadcopter detects the infected potato plants in the field and sends the GPS coordinate of these target plants to an AGV for roguing. This process is currently manual and causes significant crop loss every year. In order to reduce detection times and reduce crop loss this onboard vision system was developed. The system has a cm-level precision RTK GPS for navigation. However, even the best GPS systems still has an average error of about 10cms. This requires identification

of the plant by the rover in real-time. This will help reduce false positives. We used HSL color space to improve the accuracy of the system for finding the range of green color and working in various levels of light. Two different methods for plant detection were presented and compared. The algorithms developed reduce the error to about 2.8 to 2.9cms. Finally, the most accurate method, algorithm which was based on (fill in the method B details here) was selected after thorough screening and testing .

REFERENCES

- [1] J.G.A. Barbedo. A review on the main challenges in automatic plant disease identification based on visible range images, 2016. In *Biosystems engineering*, 144, pp.52-60.
- [2] S.S. Chouhan, U.P. Singh, and S. Jain. Applications of computer vision in plant pathology: a survey, 2020. *Archives of computational methods in engineering*, 27(2), pp.611-632.
- [3] T. Deemyad, R. Moeller, and A. Sebastian. Chassis design and analysis of an autonomous ground vehicle (agv) using genetic algorithm, 2020. In *Intermountain Engineering, Technology, and Computing Conference (IETC)* (pp. 1-6). IEEE.
- [4] T. Dewi, P. Risma, Y. Oktarina, and S. Muslimin. Visual servoing design and control for agriculture robot; a review, 2018. In *International Conference on Electrical Engineering and Computer Science (ICECOS)*, Pangkal Pinang, pp. 5762, doi: 10.1109/ICECOS.2018.8605209.
- [5] G. Dhingra, V. Kumar, and H.D. Joshi. A novel computer vision based neutrosophic approach for leaf disease identification and classification, 2019. *Measurement*, 135, pp.782794.
- [6] L.M. Griffel, D. Delparte, and J. Edwards. Using support vector machines classification to differentiate spectral signatures of potato plants infected with potato virus y, 2018. *Computers and Electronics in Agriculture*, 153:318-324. doi:DOI: 10.1016/j.compag.2018.08.027.
- [7] S. Hameed and I. Amin. Detection of weed and wheat using image processing, 2018. *5th International Conference on Engineering Technologies and Applied Sciences (ICETAS)* (pp. 1-5). IEEE.
- [8] V. Kalist, P. Ganesan, B.S. Sathish, and J.M.M. Jenitha. Possiblistic-fuzzy c-means clustering approach for the segmentation of satellite images in hsl color space, 2015. In *Procedia Computer Science*, 57, pp.49-56.
- [9] A. Kapoor, S. I. Bhat, S. Shidnal, and A. Mehra. Implementation of iot (internet of things) and image processing in smart agriculture, 2016. In *International Conference on Computation System and Information Technology for Sustainable Solutions (CSITSS)*, Bangalore, pp. 21-26, doi: 10.1109/CSITSS.2016.7779434.
- [10] A.H. Kulkarni and A. Patil. Applying image processing technique to detect plant diseases, 2012. *International Journal of Modern Engineering Research*, 2(5), pp.3661-3664.
- [11] S.S. Kumar and B.K. Raghavendra. Diseases detection of various plant leaf using image processing techniques: a review, 2019. In *5th International Conference on Advanced Computing Communication Systems (ICACCS)*. (pp. 313316). IEEE.
- [12] J. Ma, X. Li, H. Wen, Z. Fu, and L. Zhang. A key frame extraction method for processing greenhouse vegetables production monitoring video, 2015. In *Computers and Electronics in Agriculture*, 111, pp.92-102.
- [13] F. Martinelli, R. Scalenghe, S. Davino, S. Panno, G. Scuderi, P. Ruisi, P. Villa, D. Stroppiana, M. Boschetti, L.R. Goulart, and C.E. Davis. Advanced methods of plant disease detection. a review, 2015. *Agronomy for Sustainable Development*, 35(1), pp.1-25.
- [14] A.I. Martyshkin, D.A. Trokoz, and I.I. Salnikov. Development and investigation of a motion planning algorithm for a mobile robot with a smart machine vision system, 2020. *International Russian Automation Conference (RusAutoCon)* (pp. 831-838). IEEE.
- [15] R. Moeller, T. Deemyad, and A. Sebastian. Autonomous navigation of an agricultural robot using rtk gps and pixhawk, 2020. In *Intermountain Engineering, Technology and Computing (IETC)* (pp. 1-6). IEEE.
- [16] T. Nishi, S. Kurogi, and K. Matsuo. Grading fruits and vegetables using rgb-d images and convolutional neural network, 2017. *Symposium Series on Computational Intelligence (SSCI)* (pp. 1-6). IEEE.
- [17] R. Pan, W. Gao, and J. Liu. Color clustering analysis of yarn-dyed fabric in hsl color space, 2009. In *WRI World Congress on Software Engineering*, Xiamen, pp. 273-278, doi: 10.1109/WCSE.2009.148.
- [18] R. Pan, W. Gao, and J. Liu. Color clustering analysis of yarn-dyed fabric in hsl color space, 2009. In *WRI World Congress on Software Engineering*, Xiamen, pp. 273-278, doi: 10.1109/WCSE.2009.148.
- [19] J.M. Roberts, K.B. Ireland, W.T. Tay, and D. Paini. Honey bee-assisted surveillance for early plant virus detection, 2018. *Annals of Applied Biology*, 173(3), pp.285-293.
- [20] C. Saravanan. Color image to grayscale image conversion, 2010. In *Second International Conference on Computer Engineering and Applications*. (Vol. 2, pp. 196-199). IEEE.
- [21] G. Saravanan, G. Yamuna, and S. Nandhini. Real time implementation of rgb to hsv/hsi/hsl and its reverse color space models, 2016. In *International Conference on Communication and Signal Processing (ICCSP)*. (pp. 0462 0466). IEEE.
- [22] M.R. Satpute and S.M. Jagdale. Color, size, volume, shape and texture feature extraction techniques for fruits: a review, 2016. *International Research Journal of Engineering and Technology (IRJET)*, 3(02).
- [23] H.K. Suh, J.W. Hofstee, and E.J. van Henten. Improved vegetation segmentation with ground shadow removal using an hdr camera, 2018. *Precision Agriculture*, 19(2), pp.218-237.
- [24] A. Wang, W. Zhang, and X. Wei. A review on weed detection using ground-based machine vision and image processing techniques, 2019. In *Computers and electronics in agriculture*, 158, pp.226-240.
- [25] T. Welsh, M. Ashikhmin, and K. Mueller. Transferring color to greyscale images, 2002. In *Proceedings of the 29th annual conference on Computer graphics and interactive techniques* (pp. 277-280).
- [26] B. Zhang, W. Huang, J. Li, C. Zhao, S. Fan, J. Wu, and C. Liu. Principles, developments and applications of computer vision for external quality inspection of fruits and vegetables: A review, 2014. *Food Research International*, 62, pp.326343.
- [27] S. Zhang, X. Wu, Z. You, and L. Zhang. Leaf image based cucumber disease recognition using sparse representation classification, 2017. In *Computers and Electronics in Agriculture*, 134:135-141.
- [28] T. Deemyad, A. Sebastian (2021) Mobile Manipulator and EOAT for In-Situ Infected Plant Removal. In: Zeghloul S., Laribi M.A., Arsicault M. (eds) *Mechanism Design for Robotics. MEDER 2021. Mechanisms and Machine Science*, vol 103. Springer, Cham. https://doi.org/10.1007/978-3-030-75271-2_29.
- [29] T. Deemyad, N. Hassanzadeh, and A. Perez-Gracia. Coupling mechanisms for multi-fingered robotic hands with skew axes. In *Mechanism Design for Robotics (MEDER)*. Springer, 2018.
- [30] T. Deemyad, O. Heidari, and A. Perez-Gracia. Singularity Design for RRSS Mechanisms. In *USCToMM Symposium on Mechanical Systems and Robotics (MSR) Conferences*. Springer, 2020.
- [31] Mortensen, A.K., Dyrmann, M., Karstoft, H., Jørgensen, R.N. and Gislum, R., 2016. Semantic segmentation of mixed crops using deep convolutional neural network. In *CIGR-AgEng Conference*, 26-29 June 2016, Aarhus, Denmark. Abstracts and Full papers (pp. 1-6). Organising Committee, CIGR 2016.
- [32] Lottes, P., Hörferlin, M., Sander, S. and Stachniss, C., 2017. Effective vision-based classification for separating sugar beets and weeds for precision farming. *Journal of Field Robotics*, 34(6), pp.1160-1178.
- [33] Potena, C., Nardi, D. and Pretto, A., 2016, July. Fast and accurate crop and weed identification with summarized train sets for precision agriculture. In *International Conference on Intelligent Autonomous Systems* (pp. 105-121). Springer, Cham.